

# Fabrication of Polysulfone Beads Containing Covalent Organic Polymer as a Versatile Platform for Efficient Iodine Capture

Nazanin Taheri, Mohammad Dinari,\* and Vahid Ramezanzade

Cite This: *ACS Omega* 2024, 9, 19071–19076

Read Online

ACCESS |



Metrics &amp; More



Article Recommendations



Supporting Information

**ABSTRACT:** Radioactive iodine poses a significant risk to human health, particularly with regard to reproductive and metabolic functions. Designing and developing highly efficient adsorbent materials for radioactive substances remain a significant challenge. This study aimed to address this issue by the fabricating polymeric beads containing covalent organic polymer (COP) as an effective method for removing iodine vapor. To achieve this, a COP was first synthesized via the Friedel–Crafts reaction catalyzed by anhydrous aluminum chloride. Then, COP-loaded polysulfone (PSf) (COP@PSf) and PSf beads were prepared using a phase separation method. The beads produced in this research have exhibited remarkable proficiency in adsorbing iodine vapor, showing an adsorption capacity of up to 216 wt % within just 420 min, which is higher than that of most other similar beads reported in the literature.



## INTRODUCTION

Radioactive iodine in two isotopic forms, i.e.,  $^{129}\text{I}$  and  $^{131}\text{I}$ , is considered a potential threat to the environment, animals, and human health. They are highly toxic, mobile, volatile, and soluble in aqueous media.<sup>1,2</sup> Moreover, exposure to  $^{129}\text{I}$  and  $^{131}\text{I}$  is also harmful because they can disturb the metabolic activities. Strictly speaking, if iodine isotopes are transferred into the human body through polluted air, contaminated food, water, etc., they can cause metabolic dysfunction and thyroid cancer due to abnormal function of the thyroid gland.<sup>3–5</sup> One common way employed in the adsorption of iodine vapor involves using liquid solutions. However, this method can be expensive and can also damage equipment because it requires the use of highly corrosive solutions. Therefore, the use of solid adsorbents has gained considerable interest. Traditional solid adsorbents employed in iodine capture include activated carbon, silver-impregnated alumina, zeolite, and others, which are selected for their high surface area and pore size. However, their application has been limited due to issues, such as low adsorption capacity, reduced performance by increasing the temperature, sensitivity to organic contaminants, humidity, and so on.<sup>6</sup> Therefore, there is a pressing need to develop materials with a high capacity for adsorption of iodine molecules. COPs with an alluring architecture, large volume of pores, high surface area, and immense porosity can be considered as promising candidates for iodine adsorption.<sup>7–13</sup> Actually, COPs interact with the guest species in both the surface and bulk sections. Furthermore, their porous frameworks can be functionalized using multiple chemical reagents

to improve their features and performances in various applications.<sup>14–17</sup>

A variety of COPs have been synthesized and employed as iodine adsorbents. Very recently, Das et al.<sup>18</sup> reported the salt-melt polycondensation of 2,5-dimethoxy terephthalonitrile to synthesize a nitrogen/oxygen-doped nanoporous COP with the surface area of 2731 m<sup>2</sup>/g and an iodine uptake capacity as high as 5.78 g/g. Zhang et al.<sup>19</sup> developed four polymers for iodine capture through the Friedel–Crafts alkylation reaction based on triazine, perylene, and carbazole building blocks. The results showed that the adsorbent synthesized via the reaction between carbazole and cyanuric chloride (nitrogen containing units) had a higher adsorption capacity than the reference nitrogen-free one. In fact, the existence of nitrogen-rich building blocks within the structure could effect the polarity of the polymeric framework and also the charge transfer. Nitrogen atoms with lone pair electrons within the framework of the porous adsorbent give it the characteristics of a Lewis base. This property improves its attraction toward the iodine molecule (a Lewis acid), resulting in the formation of a stable state. As the iodine molecules are adsorbed onto the porous adsorbent, they can create an outer charge complex through

**Received:** December 10, 2023

**Revised:** March 9, 2024

**Accepted:** March 14, 2024

**Published:** April 2, 2024



**Table 1. Preparation Conditions of Polymeric Beads**

polymeric bead code	PSf concentration (wt %)	COP concentration (wt %)	PVA concentration (wt %)	DMF concentration (wt %)
PSf	10	0	3	87
COP@PSf (0.5:1)	10	5	3	82
COP@PSf (0.7:1)	10	7	3	80
COP@PSf (1:1)	10	10	3	77

the transfer of charges between the lone pair orbital ( $n$ ) of the nitrogen atoms in the framework and the antibonding molecular orbital ( $\sigma^*$ ) of iodine. This outer charge complex subsequently undergoes a transition to form an inner charge complex, allowing for the adsorption of additional iodine molecules and leading to the formation of a polyiodide ion complex. Therefore, the formation of effective host–guest interactions is guaranteed. In 2019, the successful synthesis of three different carbazole-based COPs with tunable morphologies via a simple Friedel–Crafts reaction was also reported by Yu et al.<sup>20</sup> for addressing environmental issues, specially iodine capture. These carbazole-based COPs provided effective binding sites and improved the affinity between the framework of the COPs and iodine molecules. In a research work conducted by Sun et al.,<sup>21</sup> thiophene-based COPs were constructed via the palladium-catalyzed Sonogashira–Hagihara cross-coupling reaction and revealed an attractive adsorption capacity for the removal of iodine molecules due to the  $\pi$ -conjugated network structure. Guanidinium-based COP (TGDM) with ionic sites bonded to iodine molecules was documented by Zhang et al.<sup>22</sup> to effectively adsorb iodine molecules with an adsorption capacity of 30 wt %.

In light of the above literature survey, it can be concluded that a promising polymeric adsorbent for iodine vapor is supposed to possess a porous structure with a high density of effective  $I_2$  binding sites, specially heteroatoms and electron rich  $\pi$ -conjugated frameworks as well as high chemical and thermal stability.<sup>20,23–26</sup> While previous studies have demonstrated the impressive performance of COPs, their incorporation into macroscopic superstructures like beads can be useful for real-world applications. With this background, this study aims to fabricate polymeric beads containing COP as efficient adsorbents for iodine vapor removal. For this purpose, first, a COP was synthesized via a Friedel–Crafts reaction between cyanuric chloride and triphenylmethane under catalysis of anhydrous aluminum chloride. Next, COP-loaded polysulfone (PSf) beads (COP@PSf) were prepared through the phase separation method via injection of the PSf solution containing COP into the coagulation bath composed of water and ethanol. COP-free PSf beads and COP in powder form were prepared for comparison. The iodine adsorption capacities and kinetics were evaluated for both beads, and a clear improvement due to the incorporation of COP was observed. The interaction between the adsorbent and iodine was studied by Raman spectroscopy.

## EXPERIMENTAL SECTION

**Materials.** Polysulfone (PSf) (reagent grade,  $\geq 98\%$ ) was purchased from China Barseell Co. Ltd. Other materials, including poly(vinyl alcohol) (PVA,  $\geq 90\%$ ), triphenylmethane, cyanuric chloride, aluminum chloride anhydrous ( $AlCl_3$ ),  $N,N$ -dimethylformamide (DMF), dichloromethane (DCM), tetrahydrofuran (THF), methanol (MeOH), and ethanol, were purchased from Honeywell.

**Synthesis of COP.** A 100 mL round-bottom flask was charged with cyanuric chloride (0.936 g, 5 mmol), anhydrous aluminum chloride (4.800 g, 36 mmol), and DCM (30 mL). The suspension was stirred under reflux at 35 °C for 30 min. Next, triphenylmethane (1.221 g, 5 mmol) was dissolved in DCM (30 mL) and then added dropwise to the first solution. The reaction mixture was stirred under reflux at 40 °C for 24 h. When the reaction was completed, a dark brown powder was obtained. The powder was sequentially washed with DCM, THF, MeOH, DMF, and water to remove unreacted monomers and oligomers. Then, the obtained solid (COP) was washed with THF in a Soxhlet extraction apparatus for 24 h. Finally, COP was vacuum dried at 80 °C for 12 h.<sup>12</sup>

**Preparation of PSf Beads Containing COP.** COP@PSf and PSf beads with different COP concentrations were prepared, as detailed in Table 1. To this end, the specific weight of PSf granules was completely dissolved in DMF under magnetic stirring at 60 °C for 24 h to obtain a homogeneous solution. Then, the prepared COP was added to the PSf/DMF solution and stirred for 24 h at 60 °C. Next, as shown in Figure 1, by using a plastic pipet, the obtained colloidal polymer



**Figure 1.** Schematic representation of the procedure for the preparation of polymeric beads.

solution containing COP was dropped into the coagulation bath composed of water and ethanol (1:1v/v) mixture as nonsolvent. Solid beads were formed as a result of a solvent (DMF)–nonsolvent (water and ethanol) exchange. To complete the removal of DMF from the prepared beads, they were immersed in a water bath overnight. Finally, the polymeric beads were dried under a vacuum at 80 °C for 24 h.

**Characterization.** Carbon dioxide ( $CO_2$ ) adsorption measurements were performed using a Belsorp Max device. For this purpose, polymeric beads (50 mg) were activated at 120 °C under a vacuum for 12 h. The surface area of the synthesized COPs was calculated using the Langmuir method. The surface morphology of the polymeric beads was checked using scanning electron microscopy (SEM) (FEI Teneo) at an accelerating voltage of 15 kV. The thermal stability of the beads was evaluated based on thermogravimetric analysis

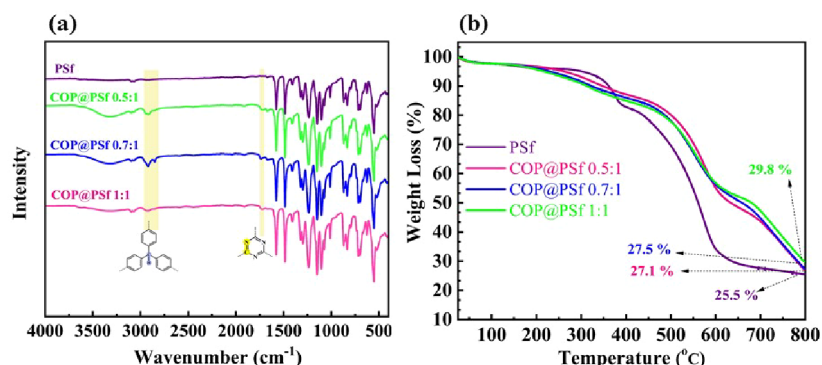


Figure 2. (a) FTIR spectra and (b) TGA thermogram of the polymeric beads.

(TGA) (TA Q-Series TGA Q500) under a nitrogen atmosphere at the heating rate of 10 °C/min. The polymeric beads were also evaluated by Fourier transform infrared spectroscopy (FTIR, PerkinElmer) in the wavenumber range of 400–4000  $\text{cm}^{-1}$ . The number of scans and wavenumber resolution was selected as 16 and 2  $\text{cm}^{-1}$ , respectively. Powder X-ray diffraction (PXRD) patterns of the samples were obtained using a Bruker D8 Discover system with a Cu  $K_{\alpha}$  source at 40 kV and 40 mA. The Raman spectrum (PerkinElmer equipped with a 532 nm diode laser) was used to determine the binding mode of iodine molecules with beads.

**Capture of Iodine Vapor Using PSf Beads Containing TPM-COP.** Certain amounts of the prepared polymeric beads (0.01 g) were placed in an opened vial (5 mL) located in another sealed vial (40 mL) containing excess iodine. Then, the whole vial was heated to 80 °C in an oven. After a period of time, the container was cooled to 25 °C and the vial containing polymeric beads was weighed very quickly. The percentage of iodine uptake ( $W$ ) was obtained using Eq 1.<sup>27</sup>

$$W = \frac{(m_2 - m_1)}{m_0} \times 100 \quad (1)$$

where  $m_1$  and  $m_2$  are the weight of the vial before and after exposure to the iodine vapor, respectively. All iodine adsorption experiments were repeated to ensure repeatability.

## RESULTS AND DISCUSSION

### Characterization of the Prepared COP@PSf Beads.

Polymeric beads were formed through a phase separation method via injection of the polymer solution containing COP into the coagulation bath containing a nonsolvent (mixture of water/ethanol 1:1 v/v). By dissolving the polymer in a solvent, a thermodynamically stable solution is obtained. When the thermodynamic stability of the solution is disturbed by some factors, the solution goes through a path of retrieving its thermodynamic stability. This path ends with phase separation into two coexisting phases, i.e., solvent-rich and polymer-rich phases. The latter forms a matrix within which the solvent-rich phases are populated. In fact, the solvent-rich phases finally turn into pores. Nonsolvent addition to the solution is one of the factors disrupting the solution's thermodynamic equilibrium. The addition of nonsolvents results in a reduction in the thermodynamic quality of the solvent, and therefore, phase separation is triggered. Under these conditions, depending on the phase separation mechanism, different structures are produced.<sup>28,29</sup>

The structure and properties of polymeric beads (COP@PSf) were characterized by FT-IR spectra, TGA thermograms, PXRD patterns, and SEM images. Figure 2a displays the FTIR spectra of the COP@PSf polymeric beads. The spectrum of the PSf bead exhibits multiple peaks, such as the symmetric and asymmetric stretching vibrations of O=S=O (1100 and 1245  $\text{cm}^{-1}$ , respectively), and C–O–C (1008 and 1146  $\text{cm}^{-1}$ , respectively). Additionally, the absorption bands at 1470 and 1590  $\text{cm}^{-1}$  correspond to the stretching vibration of aromatic C=C.<sup>27,28</sup> The FTIR spectra of the COP@PSf beads showed a new peak at 1640  $\text{cm}^{-1}$  originating from the C=N stretching vibrations of the incorporated COP. Furthermore, the C–H stretching vibration of refer to the COP monomer' can be observed within the 2850–2930  $\text{cm}^{-1}$  range (see Figure S1 for the FTIR of the COP).

The obtained TGA thermograms for the prepared beads containing different contents of COP are shown in Figure 2b. It can be observed that by increasing the COP content, the polymer bead's thermal stability slightly improves. Irrespective of the COP content, the amorphous structure of the prepared polymeric beads was deduced using the PXRD patterns shown in Figure S2. The incorporation of the COP into the PSf beads also leads to a significantly increased Langmuir surface area because of the inherent porosity of the COP (Figure S3 and Table S1).

The interior morphology of the polymeric beads was observed by using SEM images shown in Figure 3. As evident, the cross-section of beads is constructed from cellular pores, irrespective of the COP content within the bead structure. The formation of a porous morphology can be described by the phase separation of the polymer solution into polymer-rich and solvent-rich phases, as discussed above.

**Iodine Vapor Capture and Release.** To study the performance of COP@PSf beads in iodine vapor capture, a series of time-resolved experiments were performed. The results are plotted in Figure 4. Evidently, the iodine uptake and capacity of all COP@PSf beads is higher than that of neat PSf bead, and a clear positive correlation between the COP wt % and iodine uptake was observed. Additionally, the amount of adsorbed iodine significantly increases at a high rate within the first 180 min, after which the adsorption slows down. In fact, after 420 min, no remarkable change in adsorption capacity is observed, and the curve reaches a plateau, indicating the equilibrium adsorption. The equilibrium adsorption capacities were 926, 1351, 1610, and 2161 mg/g for PSf, COP@PSf (0.5:1), COP@PSf (0.7:1), and COP@PSf (1:1), respectively. In addition, when the iodine adsorption process is accomplished, the color of the polymeric beads obviously changes to

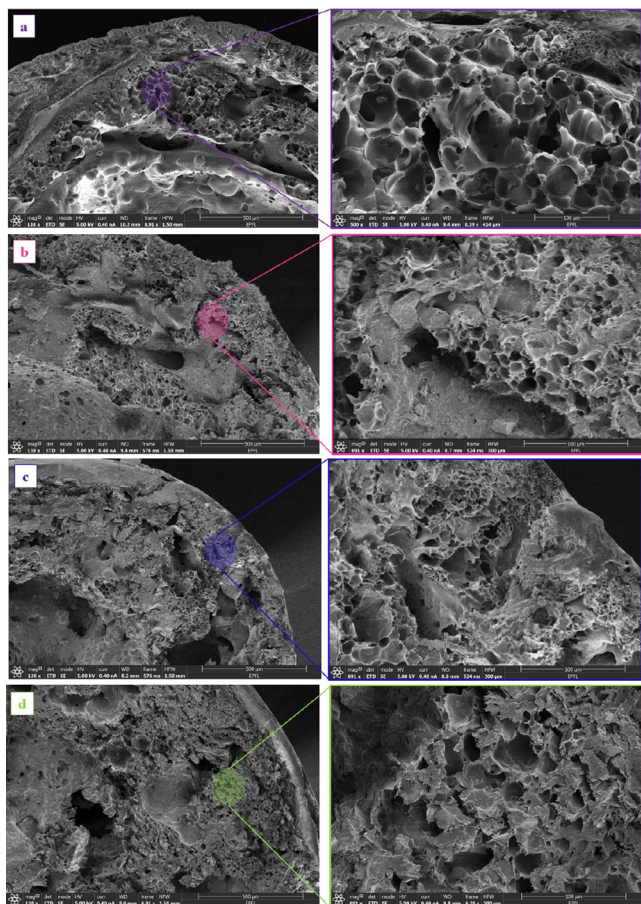


**Figure 3.** SEM images taken from the cross-section of polymeric beads: (a) PSf, (b) COP@PSf 0.5:1, (c) COP@PSf 0.7:1, (d) COP@PSf 1:1.

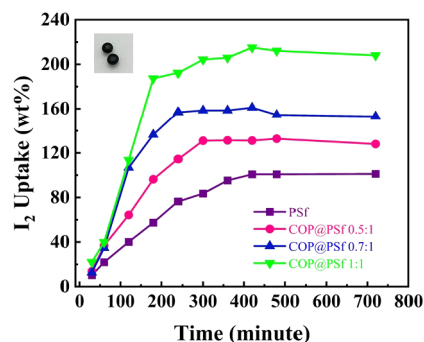


**Figure 4.** Time-resolved adsorption of the prepared polymeric beads at 80 °C in saturated iodine vapor (inset: photograph of polymeric beads after exposure to the iodine vapor for 420 h).

black (see the inset of Figure 4). In order to evaluate the performance of the COP in its powdered form and to show its positive effect on lead adsorption, the iodine adsorption experiment was conducted with powdered COP. The obtained results are shown in Figures S4 and S5. The data indicated that COP reached an iodine uptake of 2900 mg/g in 4 h. Given that bare PSf has the adsorption capacity of 926 mg/g, it can be concluded that incorporation of COP into the PSf matrix not only leads to increased porosity of polymeric beads but also improves noticeably the iodine capture capacity.

The final iodine uptake improved obviously with different loadings of COP and reached around 216 wt % after 420 min for COP@PSf (1:1) with the highest amount of COP (92.6, 135.1, and 161 wt % for the PSf, COP@PSf (0.5:1), and COP@PSf (0.7:1), respectively). In Table 2, the maximum

**Table 2.** Iodine Adsorption Capacity of Different Adsorbents

	adsorption capacity (wt %)	equilibrium time (min)		ref.
Cu-BTC@PES	63.9	72 h	bead	30
HKUST-1@PVDF	22.5	350 h	bead	31
HKUST-1@PES	37.6	350 h	bead	32
HKUST-1@PEI	34.8	350 h	bead	33
MOF-808@PVDF	142	24 h	bead	31
ZIF-8@PAN	64.3	38 h	bead	30
Bi <sub>2</sub> S <sub>3</sub> @PAN	98.6	10 h	bead	32
PHCP@PES	18.6	1 h	bead	33
COP@PSf 1:1	216	7 h	bead	this work
HCPs	257	10 h	powder	34
HDOBD	447	70 h	powder	35
FcTz-POP	396	7 h	powder	36
TatPOP-2	450	7 h	powder	37
COP	290	7 h	powder	this work

adsorption capacity and adsorption time of COP@PSf (1:1) are compared with those of beads prepared and investigated in the literature. Data in Table 2 confirm the superior adsorption of COP@PSf (1:1) prepared in this work.

The iodine captured via the polymeric beads was released by heating them at 100 °C. The results show ultrafast iodine desorption for the first 10 min, after which the adsorption becomes slow (Figure 5). After 100 min, more than 85 wt % of the adsorbed iodine was desorbed, indicating that iodine adsorption by COP@PSf beads is reversible.

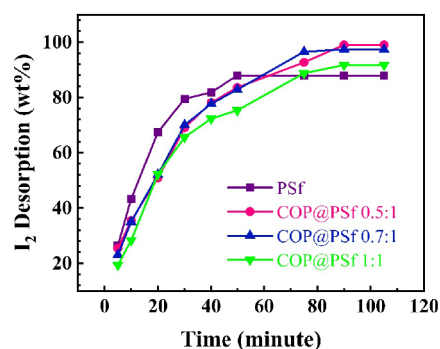


**Figure 5.** Gravimetric iodine desorption as a function of time at 100 °C.

**Iodine Adsorption Mechanism.** Considering the iodine adsorption investigated in previously published research works, nitrogen, oxygen, and sulfur atoms existing in the structure can effectively contribute to iodine capture via charge transfer at the very beginning of the adsorption process. Moreover, benefiting from the extended  $\pi$ -conjugated networks in the adsorbent structure would also cause forceful interactions with iodine molecules, and therefore, an increase in iodine

adsorption.<sup>18,33,38–43</sup> Herein, we hypothesized that the nitrogen atoms of triazine rings with their lone pair electrons act as Lewis bases, which strengthen the affinity of polymeric beads toward the iodine molecules (Lewis acid) and cause a stable state to occur. Moreover, the captured iodine molecules on the surface of the COP@PSf beads could form a charge complex by charge transfer between nitrogen's lone pair electrons ( $n$ ) and the antibonding iodine molecular orbital ( $\sigma^*$ ) ( $n \rightarrow \sigma^*$ ). Then, through a transition, the outer charge complex forms an inner charge complex, which yields more adsorption of iodine and formation of the polyiodide ion complex.

Raman spectroscopy was performed to confirm the presence of polyiodides in the beads. As shown in Figure 6, after iodine

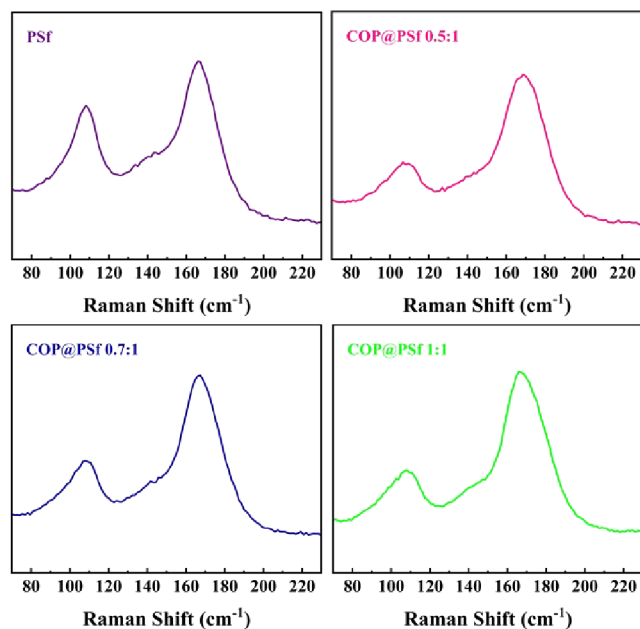


Figure 6. Raman spectra of iodine-loaded beads.

adsorption onto the surface of beads, two peaks appeared at 108 and 167  $\text{cm}^{-1}$ , which are assigned to the stretching vibrations of  $\text{I}_3^-$  and  $\text{I}_5^-$  species, respectively. Moreover, the absence of a peak at 180  $\text{cm}^{-1}$  indicates that the adsorbed iodine does not exist as molecular iodine ( $\text{I}_2$ ),<sup>20,44,45</sup>

## CONCLUSION

In summary, COP was synthesized using a simple one-step Friedel–Crafts reaction, followed by introducing the COP into the PSf matrix using a phase separation method to produce polymeric beads with varying amounts of COP loading. The final uptake of iodine was notably enhanced with varying levels of COP loading and reached a maximum of approximately 216 wt % after 420 min for COP@PSf (1:1), which had the highest concentration of COP. Incorporating COP into the PSf matrix enhanced the affinity of polymeric beads for iodine, resulting in an increased capacity for iodine capture. This was attributed to the presence of heteroatoms and electron-rich aromatic rings, which created abundant active binding sites and facilitated the efficient adsorption of iodine molecules. Additionally, the results from the iodine release experiments indicate that iodine capture by these polymeric beads is reversible.

## ASSOCIATED CONTENT

### Supporting Information

The Supporting Information is available free of charge at <https://pubs.acs.org/doi/10.1021/acsomega.3c09869>.

The FTIR spectra, PXRD plots, and the Langmuir plots of polymeric beads and COP (PDF)

## AUTHOR INFORMATION

### Corresponding Author

Mohammad Dinari – Department of Chemistry, Isfahan University of Technology, Isfahan 8415683111, Iran; [orcid.org/0000-0001-5291-7142](https://orcid.org/0000-0001-5291-7142); Email: [dinari@iut.ac.ir](mailto:dinari@iut.ac.ir)

### Authors

Nazanin Taheri – Department of Chemistry, Isfahan University of Technology, Isfahan 8415683111, Iran  
Vahid Ramezanzade – Department of Chemistry, Isfahan University of Technology, Isfahan 8415683111, Iran; [orcid.org/0000-0003-2241-3933](https://orcid.org/0000-0003-2241-3933)

Complete contact information is available at: <https://pubs.acs.org/10.1021/acsomega.3c09869>

### Notes

The authors declare no competing financial interest.

## ACKNOWLEDGMENTS

The authors gratefully acknowledge the Iranian National Science Foundation (INSF) for their financial (Grant No. 4026090) support and the Research Affairs Division of the Isfahan University of Technology (IUT) for partial financial support.

## REFERENCES

- Yu, C.-X.; Li, X.-J.; Zong, J.-S.; You, D.-J.; Liang, A.-P.; Zhou, Y.-L.; Li, X.-Q.; Liu, L.-L. Fabrication of Protonated Two-Dimensional Metal–Organic Framework Nanosheets for Highly Efficient Iodine Capture from Water. *Inorg. Chem.* **2022**, *61* (35), 13883–13892.
- Li, M.; Zhao, H.; Lu, Z.-Y. Highly Efficient, Reversible Iodine Capture and Exceptional Uptake of Amines in Viologen-Based Porous Organic Polymers. *RSC Adv.* **2020**, *10* (35), 20460–20466.
- Shetty, D.; Raya, J.; Han, D. S.; Asfari, Z.; Olsen, J.-C.; Trabolsi, A. Lithiated Polycalix[4]Arenes for Efficient Adsorption of Iodine from Solution and Vapor Phases. *Chem. Mater.* **2017**, *29* (21), 8968–8972.
- Jie, K.; Zhou, Y.; Li, E.; Li, Z.; Zhao, R.; Huang, F. Reversible Iodine Capture by Nonporous Pillar[6]Arene Crystals. *J. Am. Chem. Soc.* **2017**, *139* (43), 15320–15323.
- Tesfay Reda, A.; Pan, M.; Zhang, D.; Xu, X. Bismuth-Based Materials for Iodine Capture and Storage: A Review. *J. Environ. Chem. Eng.* **2021**, *9* (4), 105279.
- Nandanwar, S. U.; Coldsnow, K.; Utgikar, V.; Sabharwall, P.; Eric Aston, D. Capture of Harmful Radioactive Contaminants from Off-Gas Stream Using Porous Solid Sorbents for Clean Environment – A Review. *Chem. Eng. J.* **2016**, *306*, 369–381.
- Pan, X.; Ding, C.; Zhang, Z.; Ke, H.; Cheng, G. Functional Porous Organic Polymer with High S and N for Reversible Iodine Capture. *Microporous Mesoporous Mater.* **2020**, *300*, 110161.
- Hassan, A.; Alam, A.; Ansari, M.; Das, N. Hydroxy Functionalized Triptycene Based Covalent Organic Polymers for Ultra-High Radioactive Iodine Uptake. *Chem. Eng. J.* **2022**, *427*, 130950.
- Khosravi Esmailtarkhani, F.; Dinari, M.; Mokhtari, N. Nitrogen-rich Porous Organic Polymer as a Promising Adsorbent for Iodine Capture from Organic Solvents. *New J. Chem.* **2024**, *48*, 1943–1951.
- Jie, K.; Chen, H.; Zhang, P.; Guo, W.; Li, M.; Yang, Z.; Dai, S. A Benzoquinone-Derived Porous Hydrophenazine Framework for

Efficient and Reversible Iodine Capture. *Chem. Commun.* **2018**, *54* (90), 12706–12709.

(11) Taheri, N.; Dinari, M.; Asgari, M. Recent Applications of Porous Organic Polymers Prepared via Friedel–Crafts Reaction under the Catalysis of AlCl<sub>3</sub>: A Review. *ACS Appl. Polym. Mater.* **2022**, *4* (9), 6288–6302.

(12) Taheri, N.; Dinari, M. Development of Sulfonic Acid-Functionalized Covalent Organic Polymer towards Efficient Adsorption of Cationic Dyes. *Appl. Surf. Sci. Adv.* **2023**, *18*, 100543.

(13) Taheri, N.; Dinari, M. Amino-Functionalized Magnetic Porous Organic Polymer for the Selective Removal of Toxic Cationic Dyes from Textile Wastewater. *New J. Chem.* **2022**, *46* (23), 11174–11184.

(14) Das, S.; Heasman, P.; Ben, T.; Qiu, S. Porous Organic Materials: Strategic Design and Structure–Function Correlation. *Chem. Rev.* **2017**, *117* (3), 1515–1563.

(15) Tan, L.; Tan, B. Hypercrosslinked Porous Polymer Materials: Design, Synthesis, and Applications. *Chem. Soc. Rev.* **2017**, *46* (11), 3322–3356.

(16) Sun, Q.; Aguila, B.; Song, Y.; Ma, S. Tailored Porous Organic Polymers for Task-Specific Water Purification. *Acc. Chem. Res.* **2020**, *53* (4), 812–821.

(17) Mokhtari, N.; Dinari, M. Developing Novel Amine-Linked Covalent Organic Frameworks Towards Reversible Iodine Capture. *Sep. Purif. Technol.* **2022**, *301*, 121948.

(18) Das, M.; Sarkar, S. K.; Patra, Y. S.; Manna, A.; Mukherjee, S.; Das, S. Soft Self-Templating Approach-Derived Covalent Triazine Framework with Bimodal Nanoporosity for Efficient Radioactive Iodine Capture for Safe Nuclear Energy. *ACS Appl. Nano Mater.* **2022**, *5* (7), 8783–8793.

(19) Zhang, Y.; Yi, D.; Tu, P.; Yang, S.; Xie, Q.; Gao, Z.; Wu, S.; Yu, G. Boosting Radioactive Iodine Capture of Microporous Polymers through Strengthened Host–Guest Interaction. *Microporous Mesoporous Mater.* **2021**, *321*, 111148.

(20) Xiong, S.; Tang, X.; Pan, C.; Li, L.; Tang, J.; Yu, G. Carbazole-Bearing Porous Organic Polymers with a Mulberry-Like Morphology for Efficient Iodine Capture. *ACS Appl. Mater. Interfaces* **2019**, *11* (30), 27335–27342.

(21) Ren, F.; Zhu, Z.; Qian, X.; Liang, W.; Mu, P.; Sun, H.; Liu, J.; Li, A. Novel Thiophene-Bearing Conjugated Microporous Polymer Honeycomb-like Porous Spheres with Ultrahigh Iodine Uptake. *Chem. Commun.* **2016**, *52* (63), 9797–9800.

(22) Zhang, Z.; Dong, X.; Yin, J.; Li, Z.-G.; Li, X.; Zhang, D.; Pan, T.; Lei, Q.; Liu, X.; Xie, Y.; Shui, F.; Li, J.; Yi, M.; Yuan, J.; You, Z.; Zhang, L.; Chang, J.; Zhang, H.; Li, W.; Fang, Q.; Li, B.; Bu, X.-H.; Han, Y. Chemically Stable Guanidinium Covalent Organic Framework for the Efficient Capture of Low-Concentration Iodine at High Temperatures. *J. Am. Chem. Soc.* **2022**, *144* (15), 6821–6829.

(23) Qian, X.; Wang, B.; Zhu, Z.-Q.; Sun, H.-X.; Ren, F.; Mu, P.; Ma, C.; Liang, W.-D.; Li, A. Novel N-Rich Porous Organic Polymers with Extremely High Uptake for Capture and Reversible Storage of Volatile Iodine. *J. Hazard. Mater.* **2017**, *338*, 224–232.

(24) Ai, C.; Feng, J.; Yang, S.; Xiong, S.; Tang, J.; Yu, G.; Pan, C. Enhanced Iodine Capture by Incorporating Anionic Phosphate Unit into Porous Networks. *Sep. Purif. Technol.* **2021**, *279*, 119799.

(25) Zhou, B.; Chen, B.; Chen, S.; Feng, S.; Wang, D.; Liu, H. Engineering Functionality in Organic Porous Networks by Multicomponent Polymerization. *Macromolecules* **2021**, *54* (16), 7642–7652.

(26) Shang, Z.; Zhao, B.; Wu, Z.; Ding, Y.; Hu, A. Synthesis of Conjugated Mesoporous Hyper-cross-linked Polymers for Efficient Capture of Dibenzothiophene and Iodine | ACS Applied Materials & Interfaces. *ACS Appl. Mater. Interfaces* **2020**, *12*, 56454–56461.

(27) Zhao, Y.; Lu, W.; Zhang, Y.; Liu, X.; Sun, B. Room Temperature Synthesis of Piperazine-Based Nitrogen-Rich Porous Organic Polymers for Efficient Iodine Adsorption. *Microporous Mesoporous Mater.* **2024**, *366*, 112954.

(28) Fashandi, H.; Karimi, M. Pore Formation in Polystyrene Fiber by Superimposing Temperature and Relative Humidity of Electrospinning Atmosphere. *Polymer* **2012**, *53* (25), 5832–5849.

(29) Ghodsi, A.; Fashandi, H.; Zarrebini, M.; Abolhasani, M. M.; Gorji, M. Highly Effective CO<sub>2</sub> Capture Using Super-Fine PVDF Hollow Fiber Membranes with Sub-Layer Large Cavities. *RSC Adv.* **2015**, *5* (112), 92234–92253.

(30) Yu, Q.; Jiang, X.; Cheng, Z.; Liao, Y.; Duan, M. Porous ZIF-8@polyacrylonitrile Composite Beads for Iodine Capture. *RSC Adv.* **2021**, *11* (48), 30259–30269.

(31) Wang, L.; Chen, P.; Dong, X.; Zhang, W.; Zhao, S.; Xiao, S.; Ouyang, Y. Porous MOF-808@PVDF Beads for Removal of Iodine from Gas Streams. *RSC Adv.* **2020**, *10* (73), 44679–44687.

(32) Yu, Q.; Jiang, X.; Cheng, Z.; Liao, Y.; Pu, Q.; Duan, M. Millimeter-Sized Bi<sub>2</sub>S<sub>3</sub>@polyacrylonitrile Hybrid Beads for Highly Efficient Iodine Capture. *New J. Chem.* **2020**, *44* (39), 16759–16768.

(33) Chen, G.; Zhao, Q.; Wang, Z.; Jiang, M.; Zhang, L.; Duan, T.; Zhu, L. Pitch-Based Porous Polymer Beads for Highly Efficient Iodine Capture. *J. Hazard. Mater.* **2022**, *434*, 128859.

(34) Li, X.; Peng, Y.; Jia, Q. Construction of Hypercrosslinked Polymers with Dual Nitrogen-Enriched Building Blocks for Efficient Iodine Capture. *Sep. Purif. Technol.* **2020**, *236*, 116260.

(35) Geng, T.-M.; Wang, F.-Q.; Fang, X.-C.; Xu, H. Dual Functional N,O,P Containing Covalent Organic Frameworks for Adsorbing Iodine and Fluorescence Sensing to p-Nitrophenol and Iodine. *Microporous Mesoporous Mater.* **2021**, *317*, 111001.

(36) Wang, Y.; Tao, J.; Xiong, S.; Lu, P.; Tang, J.; He, J.; Javaid, M. U.; Pan, C.; Yu, G. Ferrocene-Based Porous Organic Polymers for High-Affinity Iodine Capture. *Chem. Eng. J.* **2020**, *380*, 122420.

(37) Xiong, S.; Tao, J.; Wang, Y.; Tang, J.; Liu, C.; Liu, Q.; Wang, Y.; Yu, G.; Pan, C. Uniform Poly(Phosphazene–Triazine) Porous Microspheres for Highly Efficient Iodine Removal. *Chem. Commun.* **2018**, *54* (61), 8450–8453.

(38) Shao, L.; Liu, N.; Wang, L.; Sang, Y.; Wan, H.; Zhan, P.; Zhang, L.; Huang, J.; Chen, J. Facile Preparation of Oxygen-Rich Porous Polymer Microspheres from Lignin-Derived Phenols for Selective CO<sub>2</sub> Adsorption and Iodine Vapor Capture. *Chemosphere* **2022**, *288*, 132499.

(39) Wang, J.; Wang, C.; Wang, H.; Jin, B.; Zhang, P.; Li, L.; Miao, S. Synthesis of N-Containing Porous Aromatic Frameworks via Scholl Reaction for Reversible Iodine Capture. *Microporous Mesoporous Mater.* **2021**, *310*, 110596.

(40) Geng, T.-M.; Liu, M.; Hu, C.; Zhu, F. Flexible Oxygen-Bridged Porous Organic Polymers for Adsorbing and Fluorescence Sensing Iodine and the Formation of Liquid Complexes of POPs-(Poly)Iodide Anions. *Macromol. Mater. Eng.* **2021**, *306* (4), 2000711.

(41) Harijan, D. K. L.; Chandra, V.; Yoon, T.; Kim, K. S. Radioactive Iodine Capture and Storage from Water Using Magnetite Nanoparticles Encapsulated in Polypyrrole. *J. Hazard. Mater.* **2018**, *344*, 576–584.

(42) Ruidas, S.; Chowdhury, A.; Ghosh, A.; Ghosh, A.; Mondal, S.; Wonanke, A. D.; Addicoat, M.; Das, A. K.; Modak, A.; Bhaumik, A. Covalent Organic Framework as a Metal-Free Photocatalyst for Dye Degradation and Radioactive Iodine Adsorption | Langmuir. *Langmuir* **2023**, *39*, 4071–4081.

(43) Li, H.; Zhang, D.; Cheng, K.; Li, Z.; Li, P.-Z. Effective Iodine Adsorption by Nitrogen-Rich Nanoporous Covalent Organic Frameworks. *ACS Appl. Nano Mater.* **2023**, *6* (2), 1295–1302.

(44) Pei, C.; Ben, T.; Xu, S.; Qiu, S. Ultrahigh Iodine Adsorption in Porous Organic Frameworks. *J. Mater. Chem. A* **2014**, *2* (20), 7179–7187.

(45) Sen, A.; Sharma, S.; Dutta, S.; Shirolkar, M. M.; Dam, G. K.; Let, S.; Ghosh, S. K. Functionalized Ionic Porous Organic Polymers Exhibiting High Iodine Uptake from Both the Vapor and Aqueous Medium. *ACS Appl. Mater. Interfaces* **2021**, *13* (29), 34188–34196.